Early Diagnosis of Parkinson's Disease based on Transcranial Sonography

Valanarasi Antony Santiagu Vaz
Department of ECE
Syed Ammal Engineering College
Ramanathapuram, TamilNadu, India.

ABSTRACT

Transcranial Sonography (TCS) plays a very significant role in the early analysis of Parkinson's disease (PD). The TCS taken in the mesencephelon region shows a discrete pattern with increase in size (hyper echogenecity) of substantia nigra in about 90% of PD patients. Generally this hyperechogenic pattern is segmented physically which can be used as PD indicator for early diagnosis. This paper proposes a novel procedure using GLCM and Multi Layer Perceptron Neural Network for the early PD risk assessment. The features are obtained by a assortment of Gabor filters, and the concert of these features is evaluated by feature selection method. At an earlier stage speckle noise is removed using spatially adaptive wiener filter. This method is well applicable with neural network toolbox in MATLAB.

General terms

Parkinson's disease, risk assessment, neural network, early diagnosis.

Keywords

GLCM, Mesencephalon, Hyperechogenic, Spatially adaptive wiener filter, Substantia nigra, TCS.

1. INTRODUCTION

Parkinson's disease (PD) is one of the most severe and recurrent neuro degenerative disorders of the central nervous system, which is characterized by a group of conditions called motor system disorders because of the loss of dopamine producing brain cells in Substantia nigra(a region of mid brain). Main symptoms of PD include quiver, or shaky in hands, arms, legs, jaw, and face; inflexibility, or firmness of the limbs and chest; bradykinesia, or slowness of movement; and postural unsteadiness, or impaired stability and management. The other symptoms include problems connected with physical senses, sleep and feelings. PD usually affects people over the age of 50, which has influenced a large part of worldwide population**.** Till now, the cause of PD is still unknown; however, it is possible to lessen symptom drastically at the beginning of the illness.

Substantia Nigra is a brain structure located in the mesencephalon (midbrain). A small region in the brain stem, just above the spinal cord (Fig. 1) is the substantia nigra (literally meaning "black substance").All activities of human body are controlled only by the Substantia Nigra. Cells within the substantia nigra (SN) produce and release a chemical called dopamine. Dopamine is a neurotransmitter to facilitate movement control and balance and is essential for the proper functioning of the central nervous system (CNS). The effective communication (transmission) of electrochemical signals from one nerve cell (neuron) to another is due to Dopamine. Dopamine released by SN neurons lands on the exterior of neurons in other brain centers, controls their booting actions and regulates the movements. The main target regions of dopamine release from the substantia nigra are called the caudate and the putamen. In PD, adequate dopamine is not produced due to the degeneration of the cells of SN. When this occurs, neurons elsewhere in the brain are no longer well regulated and do not behave in a normal manner. This results in a loss of control of activities, leading to slowed movements, shiver, and firmness. Early diagnosis is needed in PD therapy so that with the help of drugs such as levodopa the brain used to make more dopamine.

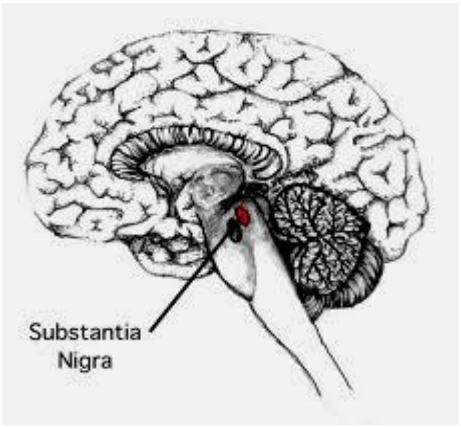

Fig.1 Position of substantia nigra

Transcranial sonography (TS) is a well established and commonly used diagnostic method in the field of neurology. With application of the color Doppler sequence, this procedure allows visualization of a noninvasive evaluation of the morphologic characteristics of several brain structures. In recent years, transcranial sonography (TCS) has evolved as a useful instrument in the differential diagnosis and even very early diagnosis of PD. As a typical characteristic, hyper echogenicity (an enlarged and more intense signal) at the anatomical site of the substantia nigra can be determined. Classification of the disease depends on the quality of the TCS images. The transcranial sonography images are rich in granule noise called speckle noise, which degrades the classification process. In this paper a novel approach is used. After image acquisition speckle noise is removed by spatially adaptive wiener filter, this is followed by feature extraction using Gabor filter and Grey Level Co-occurrence Matrices (GLCM) technique. Semi automatic method of feature

extraction is followed in this paper. Also, this paper uses the combined procedure of measuring the area of substantia nigra and extracting multiple GLCM texture features from the segmented window for PD's risk assessment. The extracted features are classified with multi layer perception neural networks there by an approximate classification rate of 96.58% can be obtained.

2. RELATED WORKS

In recent years for tissue characterization and for classification purposes the texture analysis of ultrasonic images was discovered as an effective tool. Earlier only a few attempts were employed for the textural analysis of TCS images for separation of images obtained examining the PD affected and healthy people.

C. Kier et al. [4] selected and tried geometrical moments such as moment of inertia and seven Hu moments for such classification task. The results showed that the moment of inertia and Hu1 moment could be promising image characteristics. A few limitations are 1. Only a limited number of subjects are evaluated, 2. The number of drop outs for the analysis of controls was high. 3. Manual segmentation of the ipsilateral mesencephalic brain stem is still a source of investigator dependence.

L. Chen [5, 6] combined the geometrical moments with statistical moments (mean, variance, entropy, skewness and etc.) and texture features are extracted using a cache of Gabor filter into a set of feature vectors, with aim to select the best multiple feature subset for classification. GLCM texture features are measured as well and combined with Gabor features. Support Vector Machine Classifier is used to classify the features and sequential backward selection (SBS), sequential forward selection (SFS) and sequential forward floating selection (SFFS)methods are applied to select the features to obtain the best feature subset. Authors demonstrated that 96.15% classification rate could be obtained (specificity - 94.44% and sensitivity - 97.62) using a subset consisting of five features (Hu1 moment, average contrast and three features extracted using Gabor filter). These results are really remarkable because in the order of 90% classification rate is obtained when evaluation is performed manually marking the SN area. The aim of this study is to evaluate potentiality of the textural analysis of TCS images for separation between TCS images of healthy and PD affected people trying to combine image characteristics reported before [4 – 6] with a new set of texture features. The limitation is Gabor and GLCM features greatly depend on the filter window size.

Sakalauskas et al [10] performed the texture analysis of TCS images by calculating parameters of ROI. Sequential feature selection method was applied in order to find optimal subset of features for such classification task. Linear support vector machine (SVM) classifier was used for determination of the optimal number of features for new subset. The classification rate 78.18% was obtained using the calculated texture features. MaZda free software package was used for calculation of texture parameters (features) in digitized images. It was concluded that discrimination power of these texture features is directly dependent on the image quality.

3. PROPOSED METHOD

In this section the proposed diagnostic methodology shown in Fig. 2. is described. The approach comprises of three stages. Since the TCS images are rich in speckle noise, the first stage is denoising. In the second stage feature reduction is performed using a bank of Gabor filters and GLCM. The last step defines the training and classification of the data set which is done with MLPNN model.

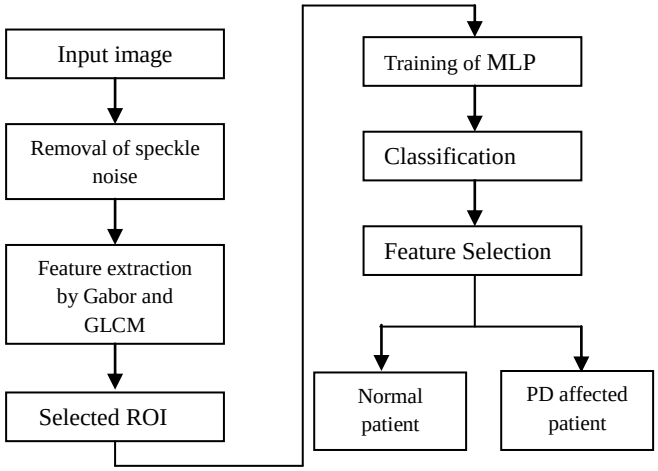

Fig.2. Structure of proposed work

3.1 Image Acquisition

Ultrasonic examination is quick to do, relatively cheap and harmless to a patient, but one of the main drawbacks of TCS examination is a poor image quality and this makes the diagnostic of neurological disorders quite subjective. The structures of interest are hardly recognizable in the obtained TCS images and only an experienced physician can identify and correctly interpret the corresponding brain structure. The quality of images is poor because the examination is performed through a relatively thin preauricular temporal bone, therefore propagation of ultrasound waves are highly affected by attenuation and refraction of non homogeneous layers of the skull bone. Also due to strongly a frequency - dependent skull bone attenuation and internal reflection, scanning is performed in a relatively low frequency range (1 – 4 MHz), thus causing the limited spatial resolution of TCS images. During scanning the physician manually outlines the SN area after acquisition of TCS image. Such marking is rather approximate, because in many cases there is no clearly seen SN area (blurred or missing boundaries), due to a poor quality of TCS images. Therefore the neuro-sonologyst who performs evaluation usually follows own intuition implying marking the possible, most probable SN area, regarding to a prior anatomical knowledge about location of the SN area respective to midbrain location. Visual evaluation of TCS images with the marked ROI showed that frequently there is no hyperechogenicity in all pixels of area outlined by the physician. Therefore such evaluation seems quite subjective. In about 90% of healthy subjects, the maximal area of SN hyperechogenicity in an axial imaging plane is below the threshold of 0.2 cm^2, whereas in PD affected persons the SN appears as a bright region interrupted by speckle noise with an area of more than 0.2 cm^2 in more than 90% of patients [11] as shown in Fig. 3.

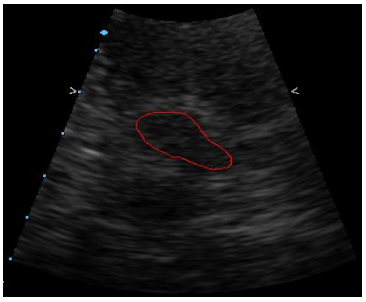

Fig.3.a. Substantia Nigra in healthy subject

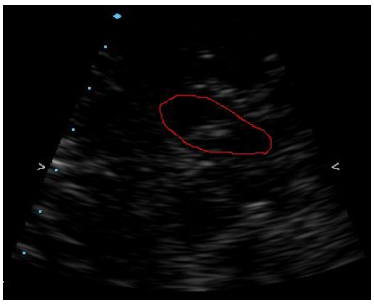

Fig.3.b. Substantia nigra in PD affected patients.

3.2 Removal of speckle noise

3.2.1. Model of Speckle Noise

Ultrasound imaging system is widely used to do the visualization of muscles, interior organs of the human body, dimension and structure and injuries. An inherent characteristic of ultrasound imaging is the presence of speckle noise. Speckle noise is a random and deterministic in an image as shown in Fig. 4. Speckle has negative impact on ultrasound imaging, drastic reduction in contrast resolution may be responsible for the poor effective resolution of ultrasound as compared to MRI.

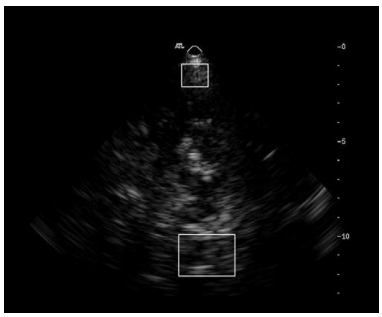

Fig. 4. Different level of speckle noise

Generalized model of the speckle [2] is represented as,

$$g(n,m) = f(n,m) * u(n,m) + \zeta(n,m) \quad (1)$$

where, $g(n,m)$ is the observed image, $u(n,m)$ is the multiplicative component and $\zeta(n,m)$ is the additive component of the speckle noise, where n and m denotes the axial and lateral indices of the image samples.
For the ultrasound imaging, only multiplicative component of the noise is to be considered and additive component of the noise is to be ignored. Hence, equation (1) can be modified as;

$$g(n,m) = f(n,m) * u(n,m) + \zeta(n,m) - \zeta(n,m)$$
Therefore $g(n,m) = f(n,m) * u(n,m)$ (2)

3.2.2. Medical Ultrasound Speckle Pattern

Nature of Speckle pattern depends on the number of scatters per resolution cell or scatter number density. Spatial distribution and the distinctiveness of the imaging system can be divided into three classes: a) The fully formed speckle pattern occurs when many random distributed scattering exists within the resolution cell of the imaging system. Blood cells are the example of this class.
b) The second class of tissue scatters is no randomly distributed with long-range order [3]. Example of this type is lobules in liver parenchyma.
c) The third class occurs when a spatially invariant coherent structure is present within the random scatter region like organ surfaces and blood vessels [3].

3.2.3. Noise Reduction in Ultra Sound Images

Steps for the speckle noise reduction in ultra sound images are carried out as below.
a. Construct Multiplicative noise model.
b. Do the transformation of Multiplicative noise model.
c. Do Wavelet transform of noisy image.
d. Calculate variance of noise.
e. Calculate weighted variance of signal ∂.
f. Calculate threshold value λ of all pixels and sub band coefficients
g. Take inverse DWT to do the despeckling of Ultrasound images .
h. Calculate PSNR (peak signal to noise ratio) for the evaluation of the algorithm.

3.3. Feature Extraction

3.3.1. Gabor filters

Generally to minimize the dimension of the input data and to reduce the time taken by the classifier feature extraction is used. In this paper texture features are extracted by a pool of Gabor filters from the region of interest. The Gabor filters are also known as Gabor wavelets. The Gabor filters is represented by Eq. (3) where x and y represent the pixel position in the spatial domain, w_θ represents the radial center frequency, q represents the orientation of the Gabor direction, and s represents the standard deviation of the Gaussian function along the x- and y- axes where $\sigma x = \sigma y = \sigma$

$$\Psi(x,y,w_\theta,\theta) = \frac{1}{2\pi\sigma^2} e^{\frac{-((x\cos\theta+y\sin\theta)^2+(-x\sin\theta+y\cos\theta)^2)}{2\sigma^2}} \quad (3)$$

The Gabor filter can be decomposed into two different equations, one to represent the real part and another to represent the imaginary part as shown in Eq. (4) and Eq. (5) respectively

$$\Psi(x,y,w_\theta,\theta) = \frac{1}{2\pi\sigma^2} exp\left\{-\left(\frac{\acute{x}^2+\acute{y}^2}{\sigma^2}\right)\right\} * [cosw_0\,\acute{x} - e^{-(w_0^2\sigma^2)/2}] \quad (4)$$

$$\Psi(x,y,w_\theta,\theta) = \frac{1}{2\pi\sigma^2} exp\left\{-\left(\frac{\acute{x}^2+\acute{y}^2}{\sigma^2}\right)\right\} * [sinw_0\,\acute{x}] \quad (5)$$

where
$\acute{x} = x\cos\theta + y\sin\theta \;\; ; \;\; \acute{y} = -x\sin\theta + y\cos\theta$ and
$\sigma = \pi / w_0$ (6)

From the convolution of the Gabor filter parameters Ψ and *I*, Gabor features are derived.

$$C_{\Psi I} = I(x,y) * \Psi(x,y,w_0\theta) \quad (7)$$

The term $\Psi(x,y,w_0\theta)$ can be replaced by Eq(4) and Eq (5) to derive the real and imaginary parts of Eq (2) and is represented by $C^r_{\Psi I}$ and $C^i_{\Psi I}$ respectively. The real and imaginary parts are used to compute the local properties of the image using Eq (8).

$$C_{\Psi I}(x,y,w_0,\theta) = \sqrt{\|C^r_{\Psi I}\|^2 + \left\|C^i_{\Psi I}\right\|^2} \quad (8)$$

The convolution can be performed using a fast method by applying Fast Fourier Transform (FFT), Point to point multiplication and Inverse Fast Fourier Transform (IFFT). It is performed on three radical center frequencies, w_0 and eight orientations. The Gabor features are at a high-dimensional space. However, higher dimension will affect the learning of the classification. A down-sampling can be performed by omitting values from the Gabor features with a factor of ρ. The Gabor features are concatenated to form a feature vector as shown in Eq. (9).

$$C^{(\rho)} = \left(C^{(\rho)}_{\Psi I}(x,y,w_0^1,\theta^1), \ldots\ldots C^{(\rho)}_{\Psi I}(x,y,w_0^1,\theta^m)\right)^T \quad (9)$$

3.3.2. GLCM

GLCM is extensively been used for various texture analysis applications, such as texture classification, rock texture classification, wood classification and etc. The GLCM is generated by cumulating the total numbers of grey pixel pairs from the images. Each GLCM is generated by defining a spatial distance *d* and an orientation, which can be 0 degree, 45 degree, 90 degree or 135 degree at a selected grey level *G*. The GLCM produced will be of size $G \times G$.When the GLCM is constructed, $C_d(r,n)$ represents the total pixel pair value, where *r* represents the reference pixel value and *n* represents the neighboring pixel value according to the spatial distance and orientation defined. The joint probability density function normalizes the GLCM by dividing every set of pixel pairs with the total number of pixel pairs used and is represented using $p(r,n)$ as shown in Eq. (10).

$$p(r,n) = \frac{1}{\sum_{r=0}^{G-1}\sum_{n=0}^{G-1} C_d(r,n)}\, C_d(r,n) \quad (10)$$

Textural features are extracted from the GLCMs for classification process. Nearly fourteen features are normally used. The features that are used in this paper are

$$Contrast = \frac{1}{(G-1)^2}\sum_{r=0}^{G-1}\sum_{n=0}^{G-1}(r-n)^2\, p(r,n) \quad (11.a)$$

$$Homogenecity = \sum_{r=0}^{G-1}\sum_{n=0}^{G-1}\frac{p(r,n)}{(1+|r-n|)} \quad (11.b)$$

$$Entropy = \sum_{r=0}^{G-1}\sum_{n=0}^{G-1} p(r,n)\log p(r,n) \quad (11.c)$$

$$Energy = \sum_{r=0}^{G-1}\sum_{n=0}^{G-1} p(r,n)^2 \quad (11.d)$$

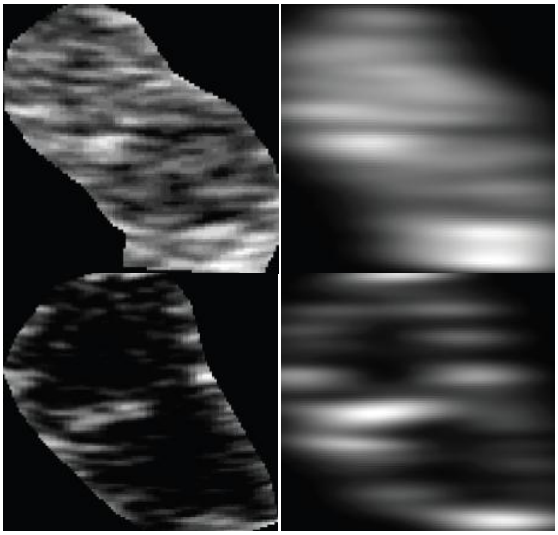

(c) (d)

Fig.3.aROI in a healthy subject b.Gabor filter with cale0 c.ROI in PD affected subject d. Gabor filter with scale 0

3.4. Classification based on MLPNN

3.4.1. MLP Neural Network

A multilayer perceptron is constructed by connecting a number of neurons in layers which are able to solve non linearly separable problems. Each of the perceptrons is used to identify small linearly separable sections of the inputs.Outputs of the perceptrons are combined into another perceptron to produce the final output. In a multilayer perceptron, the neurons are arranged into an input layer, an output layer and one or more hidden layers.

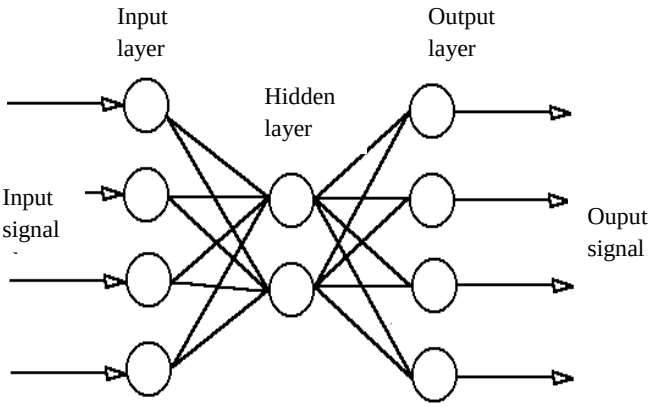

Fig. 4. The multilayer perceptron model

The learning rule for the multilayer perceptron is known as "the generalized delta rule" or the "backpropagation rule". The generalized delta rule repetitively calculates an *error function* for each input and backpropagates the error from one layer to the previous one. The weights for a particular node are adjusted in direct proportion to the error in the units to which it is connected.

Let E_p=Error function for pattern *p*

t_{pj}=Target output for pattern *p* on node *j*

o_{pj}=Actual output for pattern *p* on node *j*

w_{ij}=Weight from node *i* to node *j*

The error function E_p is defined to be proportional to the square of the difference $t_{pj} - o_{pj}$.

$$E_p = \frac{1}{2} \sum_j (t_{pj} - o_{pj})^2 \quad (12)$$

The activation of each unit j , for pattern p, can be written as

$$net_{pj} = \sum_j w_{ij} o_{pi} \quad (13)$$

The output from each unit *j* is evaluated by the non-linear transfer function f_j

$$o_{pj} = f_j(net_{pj}) \quad (14)$$

It is assumed that f_j be the sigmoid function,

$$f(net) = 1/(1 + e^{-\mathbf{k}.net}) \quad (15)$$

where ***k*** is a positive constant that controls the "spread" of the function. The delta rule gear weight changes that follow the path of steepest descent on a surface in weight space. The height of any point on this surface is equal to the error measure E_p. This can be shown by screening that the derivative of the error measure with respect to each weight is proportional to the weight change dictated by the delta rule, with a negative constant of proportionality, i.e.,

$$\Delta_p w_i \propto -\partial E_p / \partial w_{ij} \quad (16)$$

3.4.2. Learning algorithm using the generalized delta rule

1. Initialize weights (to small random values) and transfer function
2. Present input
3. Adjust weights by starting from output layer and working backwards

$$w_{ij}(t+1) = w_{ij}(t) + \eta \delta_{pj} o_{pi} \quad (17)$$

$w_{ij}(t)$ represents the weights from node *i* to node *j* at time *t*, η is a gain term, and δ_{pj} is an error term for pattern *p* on node *j*.
For output layer units

$$\delta_{pj} = \mathbf{k} o_{pj}(1 - o_{pj})(t_{pj} - o_{pj}) \quad (18)$$

For hidden layer units

$$\delta_{pj} = \mathbf{k} o_{pj}(1 - o_{pj}) \sum_k \delta_{pk} w_{jk} \quad (19)$$

where the sum is over the *k* nodes in the following layer. The learning rule in a multilayer perceptron is not guaranteed to produce convergence, and it is possible for the network to fall into a situation (the so called *local minima*) in which it is unable to learn the correct output.

3.4.3. Multilayer Perceptrons as Classifiers

In MATLAB, the MLP topology is created with patternnet function with inputs and targets *patternnet(hiddenSizes,trainFcn)* with parameters of number of hidden layer and training function. In this work *hiddenSizes=3* and *trainFcn* is *traingdx.* Training set S for supervised learning is given by inputs and desired response (targets).

$$S=\{(I_1, D_1), (I_2, D_2), \ldots, (I_n, D_n)\} \quad (20)$$

The input for the MLPNN is vectors with optimal position of ellipses for different input images, The desired responses are given as positions of correct coordinates for ellipse. The goal of ANN module is a learning of position for different images which is based on correct SN position in input image (Fig. 3). Designed ANN is 3-layer MLP where hidden layer computes the positions. As outpu the correct ellipse to consecutive area measurement inside ROI is obtained. Activation function for this case is used logical sigmoid expressed by:

$$f(x) = \frac{1}{1 + e^{-\lambda x}} \quad (21)$$

where λ is gain of sigmoid $0 \leq \lambda \leq 1$, standardly λ=1. ANN compares after each epoch of leasing an error which is define as difference between targets and output from network. If this error is minimal learning can be stopped. The MSE is expressed as sum of partial differences between real results and desired response.

$$MSE = \frac{1}{N} \sum_{j=1}^{N} (D_i - I_i)^2 \quad (22)$$

Total error is defined by summation of partial errors for each training sample. Partial error for j-th training sample is defined as the difference *Dj* − *I*j. This error is computed for each sample from *S*. The goal of ANN training is to minimize MSE. MSE < 0.01 (threshold value) is reached after 100 epochs of learning. User can set a new coordinates as applicable input followed by re-train of ANN with new coordinates. These coordinates are considered as new inputs. Furthermore, downward tendency of MSE is observed. Thus *if* TMSE ≤ 0.01 *then* stop_learning *else* next epoch. Practical testing of this method showed that designed ANN is useful for positioning of ellipse in correct position in ROI window. Accuracy of this method is approximately 72% for 50 tested images. Re-training allows reaching higher accuracy for manually set of coordinates and more images as input position.

3.4.4. Module area measurement

After this processing with ANN module for correct positioning of ROI inside SN, the area of lesions (regions) for all intensities are computed. The result of this module is decreasing area depend on level of echogenicity (intensity) to distinction of PD and non-PD cases, it is based on twofold thresholding and using masks as ROI objects.

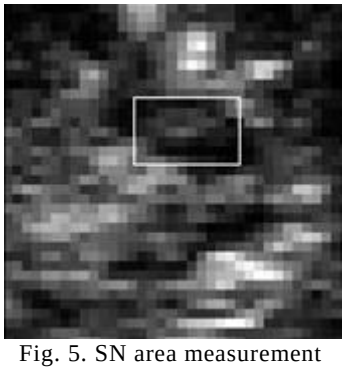

Fig. 5. SN area measurement

3.4.5. Selection of Gabor features

Given a feature vector, the goal of feature selection is to select the best feature subset automatically for classification purposes. The MLP classifier has been chosen to evaluate the effectiveness of feature subsets. The feature selection detects an optimal feature subset based on the feature vector F. A general feature selection method, sequential feature selection includes two components. First, over all possible feature subsets are minimized based on a criterion function. Another is a sequential search strategy, which establish the best feature subset. For the sequential forward selection (SFS), features are selected successively by adding the locally best feature, which is the one that provides the lowest criterion value, to an empty candidate set. By identifying the first feature that has the highest discrimination power, the SFS technique starts from the best individual feature (BIF). The SFS stop until the further features does not decrease the criterion. The sequential backward selection (SBS) method is the 'bottom up' counterpart to SFS. In SBS, starting from a full candidate set, one sequentially removes the feature which has the highest criterion until the removal of any further features may lead to an increase of the misclassification rate.

4. EXPERIMENTAL RESULTS

An experimental study has been conducted to assess whether the image features can be used as an early PD indicator. The study consisted of 36 healthy controls (subjects without mutation and symptoms of PD) and 42 Parkin mutation carriers. All these 78 subjects underwent a detailed neurological examination. Therefore the diagnosis result can be considered as the ground truth to compare and evaluate the classification. In each image the half mesencephalon (ROI marked by red contour) and even the SN (yellow contour) area was manually segmented by two individual physicians. The features which can be used to recognize the TCS images of mesencephalon of two different categories called 'healthy controls' and 'PD' are developed.. The difference of gray value distributions between these two class images can be seen more clearly. Statistical moments, geometrical moments and Gabor texture features are extracted from the images.

When statistical features, geometrical features and Gabor texture features are added successively into the feature vector the classification gives the correct rates of 79.82% and 79.67%. Then the SBS and the SFS are used, respectively, to minimize the best feature subset. Comparatively, the feature subset obtained by SFS gives the highest classification rate of 96.58%. In this feature subset, the Gabor features f (8), f (9) have the best individual performance of 89.27%. The SN area is measured and compared for the cross validation with the results obtained. The results shows that better accuracy can be obtained using this combination of the algorithms.

Table.1. Classification rate (%)

Feature set	CR %	Sensitivity	Specificity
F(1…15)	79.82	72.78	91.34
F(1…23)	79.67	72.78	91.34
SBS	93.56	85.41	97.65
SFS	96.58	95.49	97.65
Gabor f(8)	89.27	81.22	95.38
Gabor f(9)	89.27	81.22	95.38
Gabor f(4)	88.46	78.43	95.38
SN area	90.12	83.27	94.24

5. CONCLUSION

This paper concentrates on selecting good combination of features and a classifier which suits for the Parkinson's disease risk assessment based on TCS images. A hybrid feature extraction method is proposed which include statistical, geometrical and texture features for the early PD risk assessment. The classifier separate the input images into two classes by image characteristics other than the manual segmentation of substantia nigra. The SFS is implemented and three Gabor texture features were found being the best parameters to separate control subjects from parkin mutation carriers. Future work will firstly be focused on using a large number of subjects evaluated as ground truth datasets to validate the performance of selected features. Secondly the investigator dependence is to be eliminated caused by the manual segmentation of the ipsilateral mesencephalic brain stem by a semi-automatic segmentation algorithm.

6. REFERENCES

[1] Berg D., Godau J., Walter U., " Transcranial sonography in movement disorders." The Lancet Neurology. 2008. Vol. 7 (11). P.1044–1055.

[2] K. Thangavel, R. Manavalan, Laurence Aroquiaraj, "Removal of Speckle Noise from Ultrasound Medical Image based on Special Filters: Comarative study", ICGST-GVIP Journal, Vol. 9, Issue:3, pp. 25-32, June 2009.

[3] Khaled Z. AbdElmoniem, Yasser M. Kadah and AbouBakr M. Youssef, "Real Time Adaptive Ultrasound Speckle Reduction and Coherence Enhancement", 078032977/00/$10© 2000 IEEE, pp. 172-175.

[4] Kier C., Seidel G., Bregemann N., Hagenah J., Klein C., Aach T., Mertins A., "Transcranial sonography as early indicator for genetic parkinson's disease". 4th European Conference of IFMBE. 2009. P. 456-459.

[5] Chen L., Hagenah J., and Mertins A, ". Texture Analysis Using Gabor filter Based on Transcranial Sonography Image". Proceedings of 2011 Bvm bildverarbeitung fur die medizin. 2011.P. 249-253.

[6] Chen L., Seidel G., Mertins A., " Multiple Feature Extraction for E]rly Parkinson Risk Assessment Based on Transcranial Sonography Image" . Proceedings of 2010 IEEE 17th International Conference on Image Processing. 2010. P. 2277-2280.

[7] Szczypinski P., Strzelecki M., Materka A., Klepaczko A. "MaZda-A software package for image texture analysis", Computer Methods and Programs in Biomedicine. 2009. Vol. 94(1). P. 66-76.

[8] Szczypinski P., Strzelecki M., Materka A., " MaZda - a Software for Texture Analysis", Proc. of ISITC 2007, November 23-23, Republic of Korea. 2007. P. 245-249.

[9] Manjunath B.S., Ma W.Y., " Texture features for browsing and retrieval of image data" . IEEE Transactions PAMI. 1996. Vol. 18(8). P. 837 – 842

[10] A. Sakalauskas1, A. Lukoševičius, K. Laučkaitė, " Texture analysis of transcranial sonographic images for Parkinson disease ISSN 1392-2114 ULTRAGARSAS (ULTRASOUND), Vol. 66, No. 3, 2011.

[11] Walter U, Behnke S, Eyding J, et al., " Transcranial brain parenchyma sonography in movement disorders: State of

the art". Ultrasound in Medicine & Biology. 2007;33(1):15–25.

[12] http://www.ninds.nih.gov/disorders/parkinsonsdisease /parkinsons_disease.html.

[13] V. B. Rao, *C++ neural networks and fuzzy logic*: MTBooks, IDG Books Worldwide, Inc., 1995.

[14] D. Anderson and G. McNeill, "Artificial neural network technology," Rome Laboratory, New York1992.

[15] J. Tebelskis, "Speech recognition using neural networks," PhD, Carnegie Mellon University, Pittsburgh, Pennysylvania, 1995.

[16] L. Pretchelt, "Early stopping - but when?," *Neural Networks: Trick of the Trade,* vol. 1524, pp. 55-69, 1996.

[17] Weisstein, Eric W. "Levenberg-Marquardt Method", http://mathworld.wolfram.com/Levenberg- arquardt Method.html

[18] M. T. Hagan and M. B. Menhaj, "Training feedforward networks with the Marquardt algorithm," *IEEE Trans. on Neural Networks*, vol. 5, pp. 989 - 993, 1994.